On the precision of neural computation with interaural time differences in the medial superior olive

Zbynek Bures[a,b,c], Petr Marsalek[c,d,e,*]

[a] College of Polytechnics, Tolsteho 16, 586 01, Jihlava, Czech Republic
[b] Institute of Experimental Medicine, Academy of Sciences of the Czech Republic, Videnska 1083, 142 20, Praha 4, Czech Republic
[c] Czech Technical University in Prague, Zikova 1903/ 4, 166 36, Praha 6, Czech Republic
[d] Institute of Pathological Physiology, First Medical Faculty, Charles University in Prague, U Nemocnice 5, 128 53, Praha 2, Czech Republic
[e] Max Planck Institute for the Physics of Complex Systems, Nöthnitzer Strasse 38, 01187 Dresden, Germany

Abstract

We study a model of mammalian sound source localization in horizontal plane. Experiments on small rodents indicate that mammals use broadly tuned channels of azimuth for localization in horizontal plane. In mammals this neural computation is implemented by medial superior olive (MSO) for low frequency sounds. It has been shown previously that spike timing jitter, coincidence detection window length, sound frequency, among other input parameters, influence the output precision, measured by the just noticeable difference in output of the circuit. It is more difficult, if not impossible, to investigate the effect of jitter and other parameters mentioned above in electrophysiological experiment. Therefore we use previously published stochastic model with spiking neurons. We calculate properties of the model with the use of analytical methods. Predictions of the model we present here have straightforward applications in testing and designing stimulation protocols used in cochlear implants.

Abstract must be rewritten.

Keywords: binaural hearing, coincidence detection, ergodic hypothesis, ideal observer, interaural time difference, just noticeable difference, medial superior olive

Check list:

1

2

3

*Corresponding author; On leave from Prague; VoIP Telephone +420 910 116629.
Email address: Marsalek@pks.mpg.de (Petr Marsalek)

Abbreviations and symbols

C_{V}, coefficient of variation; f, f_{S}, sound frequency; F_{C}, critical sound frequency value; φ, sound phase; ILD, interaural level difference; ITD, interaural time difference; ISI, inter-spike interval; JND, just noticeable difference; LSO, lateral superior olive; K_{C}, K_{S}, A, B, C, proportionality constants; l, sound level; MSO, medial superior olive; r_{V}, VS, vector strength; R_{F}, firing rate; σ, standard deviation; T_{J}, timing jitter; t, time; T, T_{S}, sound period;

1. Introduction

Mammalian sound localization circuits contain two nuclei in the auditory brainstem, the medial and the lateral superior olive (MSO and LSO). Neurons in these nuclei are the first binaural neurons in the auditory pathway, they are connected to both ears.

This article presents description of information encoding and neural computation in the MSO obtained mostly with analytical computations. Using the analytical tools we extend quantitative results obtained by Sanda and Marsalek (2012) only in simulations and connect them to Bures and Marsalek (2013) to arrive to unified description of neural circuits in the superior olive.

Due to the physical nature of the binaural sound, the MSO neurons process spike timing differences in the range of tens of microsecond (μs). The MSO processes low frequency sounds (in human this is from 20 Hz to not more than 2 kHz). The LSO processes high frequency sounds (in human this is from 1 kHz up to 20 kHz). The overlapping region is known to have a sensitivity drop Mills (1958).

Firing rate, first spike latency and individual spike timings are used in neural system coding, especially in the auditory pathway. The highest known spike timing precision has been proven to be utilized in the mammalian auditory system, Simmons (1989). Different neural mechanisms are employed in the two nuclei.

To be continued...

Very-raw-paragraph: **In theory** It is reported (citation?) (interim citations: LSO Tollin (2003), MSO Grothe et al. (2010)...) that workings of the LSO and MSO are largely independent on sound intensity, so in theory there should not be any dependence. In contrast, since LSO and MSO extract location information with the use of different physical cues, based on the sound frequency, the sensitivity of the system to different main sound frequency should be different. **In practice** After we thoroughly studied mathematical description of our model

of the MSO circuit, we arrived to observations, which we present here in the following section of results.

First look at the data could enable us to generalize when we speed up, or slow down the system, which in principle can be done as ten times up and ten times down, see Table 2.

MSO is the largest of the nuclei and in human contains approximately 15,500 neurons, LSO contains 5600 cells.

TO-DO: rewrite this paragraph/ or put it into discussion, at the moment the text looks repetitive. The range of sound frequencies Marsalek and Kofranek (2004); Grothe et al. (2010) processed in the MSO circuit is limited to the low frequency band. In human, where audible sound frequencies range from 20 Hz to 20 kHz, this low frequency band spans from 20 Hz to 1.5 kHz. Moreover, in the marginal values of this interval, determination of sound azimuth is below the average taken through all these low frequencies. It is generally agreed that the main reason, why the workings of the MSO circuit deteriorate towards higher frequency is lowering of the synchronization of spike trains in the circuit with the sound source phase. The synchronization between two corresponding series of point events can be expressed as a (discrete version of) vector strength, defined below in equation (5).

2. Results

We investigate the dependence of the circuit output on sound frequency and sound intensity.

The degree of synchronization is measured by the vector strength measure, (5).

Figure 1 shows an example of typical vector strength lowering towards higher frequencies, as observed in the auditory nerve (AN). The prevailing majority of neurons in the auditory pathway has a vector strength spike train statistics sigmoidally dropping towards higher sound frequencies as it is in this example. In this figure, data recorded by Joris (1996) from the MSO in cat were fitted to the sigmoidal curve with the general formula of the Boltzmann function used in Marsalek and Lansky (2005). The curve fit of vector strength r_{V} is:

$$r_{\mathrm{V}} = (1 + \exp(K_{\mathrm{S}} f_{\mathrm{S}} - K_{\mathrm{C}} F_{\mathrm{C}}))^{-1}, \tag{1}$$

where K_{S} and K_{C} are parameters, proportionality constants, f_{S} is sound frequency and F_{C} is another parameter, critical half frequency.

Figure 2 shows the best JND obtained with the basic parameter set in dependence on the sound frequency. The quadratic curve fit of the JND denoted Δt_{JND} is:

$$\Delta t_{\mathrm{JND}} = A(f_{\mathrm{S}} - F_{\mathrm{C}})^2 + B, \tag{2}$$

where A and B are fitted constants and the other parameters and variables are as above. Se also Zwislocki and Feldman (1956).

Figure 3 shows existence of both a critical and an optimal values of timing jitter in respect to the attaining of the JND and output firing rate. Simulations show that with lowering timing jitter the circuit output is virtually more and more precise. The two curve fits are:

1. fit of exponential function to simulations:

$$\Delta t_{\mathrm{JND}} = \exp(A(\tau_{\mathrm{J}} - B)) - C, \tag{3}$$

where $A = 1.9$, $B = 1.25$ and $C = 0.2$ are fitted parameters.

2. Another fit, together with noise, to a quadratic function:

$$\Delta t_{\mathrm{JND}} = A(\tau_{\mathrm{J}} - B)^2 + C, \tag{4}$$

where $A = 2.5$, $B = 1$, $C = 1$, *this must be explained - that this fit is after normalization!*.

Logarithm of the JND lowers with a curve close to the square root of the jitter. This trend ends up at the critical value of jitter: $\tau_{\mathrm{J}} \approx 0.5\ ms$. Beyond that point towards the lower jitter values, the neural circuit cannot function properly, as a too low jitter prevents the interaction of spikes from the left and right side within the coincidence detection mechanism. The other (optimal) jitter value notable in this Figure 3 is a firing rate in dependency on the jitter values. This is an analytical dependency obtained in Salinas and Sejnowski (2000) for a perfect integrator model with several inputs. The mechanism studied thereof is close to the MSO neural mechanism studied here. The firing rate changes in dependency on the input spike timing variability of partially correlated input spike trains.

Figure 4 shows the calibration curve. The rising slope of this curve is used as a readout function yielding th firing rate in dependency on the ITD, which in turn signals the sound azimuth to the next nuclei up to the auditory pathway.

TO-DO - This Table 1 should be extended: more parameters and range of parameters...

Parameter	Typical Value	Ranges
$T_J = \sigma$	1 ms	0.125 - 8 ms
w_{CD}	0.6 ms	0.15 - 1.5 ms
f	200 Hz	40-1600 Hz

Table 1: The basic set of parameters.

Parameter	units	4× slower	original values	4× faster	8× faster
sound frequency	Hz	35	140	560	1120
window size	μs	2400	600	150	75
jitter	ms	4	1	0.25	0.125
Predicted JND	μs	40	10	2.5	1.25
Predicted detection time*	ms	2,600	650	162.5	81.25

Table 2: This Table is direct scaling of parameters used in Sanda and Marsalek (2012). Predicted values are: 1) just noticeable difference (JND) of the ITD 2) the time of observation by an ideal observer reading the information from one neuron.

3. Discussion

3.1. Things to do

First: Reproduce the curve in panel with sound frequency on x-axis and JND on the y-axis in Fig. 2.

Second: Present the curve from the right panel of Fig.4 from Sanda P., Jitter Effect on the Performance..., as part of Fig. 3.

Some other tentative questions: What is the highest slope of the ITD interpolation curve, such that it gives the resolution of 4° (angular degrees)?

(This we will do later: We also discuss the relation of the MSO neural circuit to its neighboring nucleus, the LSO, and its output.)

Cite: Mlynarski and Jost (2014)...

We should further discuss Sanda (2011), etc, etc...

4. Experimental Procedures

4.1. Preliminaries

Our procedures are mostly in using computational models, experimental data and statistical methods. Here we list several assumptions used in the paper.

(1) Single MSO neuron constants, see Toth and Marsalek (2015). (2) Synaptic machinery, see Toth and Marsalek (2015). (3) Ergodic assumption see Sanda and Marsalek (2012).

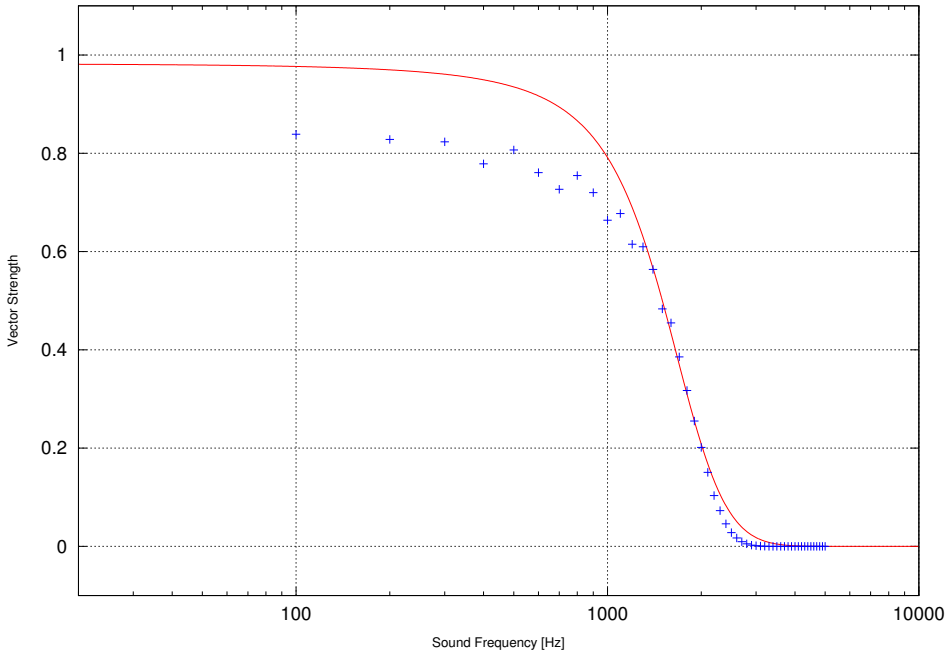

Figure 1: **Vector strength of AN spike trains in dependence on sound frequency.** X-axis shows fundamental sound frequency in Hz in a logarithmic scale and y-axis shows the vector strength. Even though is some nuclei up the auditory pathway the synchronization can be maintained towards higher frequencies than shown here, the decrease of the vector strength towards higher frequencies is a general property of all neurons in the auditory pathway.

4.2. Vector strength

The vector strength is defined as it is used since Goldberg and Brown (1969). Let us have sample (spike) phases φ_i, $i = 1, 2, \ldots, N$ relative to phases of a given input master periodic function, which does not enter the formula. (Such function can be for example sound stimulus eliciting the spike train as a response.) (Discrete sum) vector strength of sample $\varphi_1, \ldots, \varphi_N$ is defined as

$$r_{\mathrm{V}}(\varphi_i) = \frac{1}{N}\sqrt{\left(\sum_{i=1}^{N}\cos\varphi_i\right)^2 + \left(\sum_{i=1}^{N}\sin\varphi_i\right)^2}\,. \tag{5}$$

4.3. Just noticeable differences of ITD

This subsection of Methods should be analogous to the corresponding section in Bures and Marsalek (2013)...

4.4. Model of the MSO neural circuit

To do: Describe model and calculations.

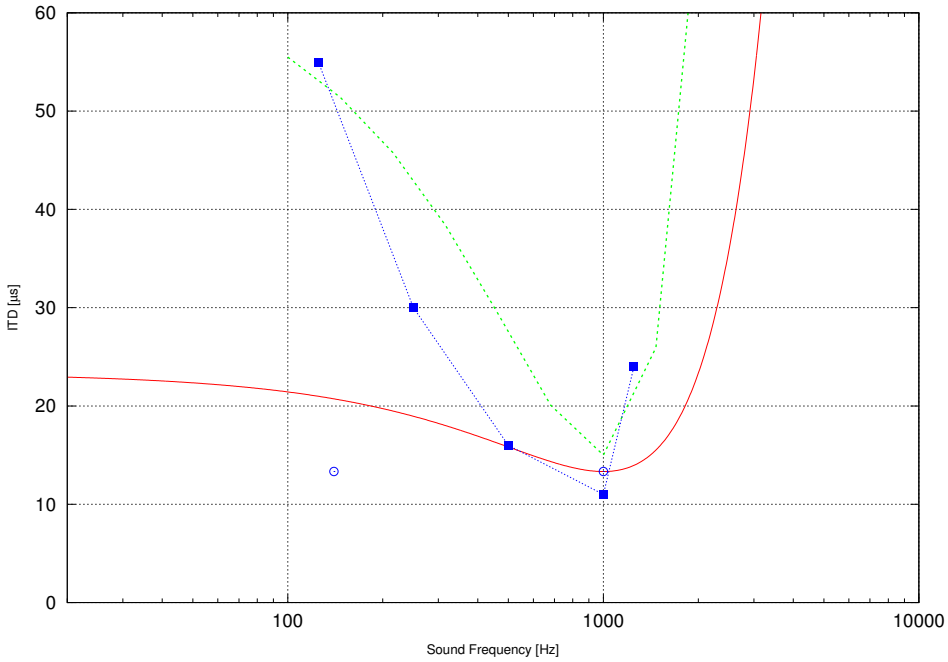

Figure 2: **The shortest ITD detected in the dependence on sound frequency.** X-axis shows sound frequency in Hz in a logarithmic scale and y-axis the shortest JND in μs. This is a theoretical prediction based on the analytical model and basic parameter set used in previous simulations.

Acknowledgments

Date is now: April 10, 2017. These were the last projects in 2013/ 2014, etc...

Supported by projects M00176 "Co-operation in biomedicine and electronics" and "Support of individual careers of prospective academic workers" to Z.B. at the College of Polytechnics Jihlava and by a graduate students' research program of Charles University SVV - 2015 - 260157, PRVOUK ?

Notes

To Do: Look at:

Kerber S., Seeber B.U. Sound localization in noise by normal-hearing listeners and cochlear implant users. Ear Hear. 2012 Jul-Aug;33(4):445-57.

References

Bures, Z., 2012. The stochastic properties of input spike trains control neuronal arithmetic. Biol. Cybern. 106 (2), 111–122.

Bures, Z., Marsalek, P., 2013. On the precision of neural computation with the interaural level difference in the lateral superior olive. Brain Res. 1536, 111–122.

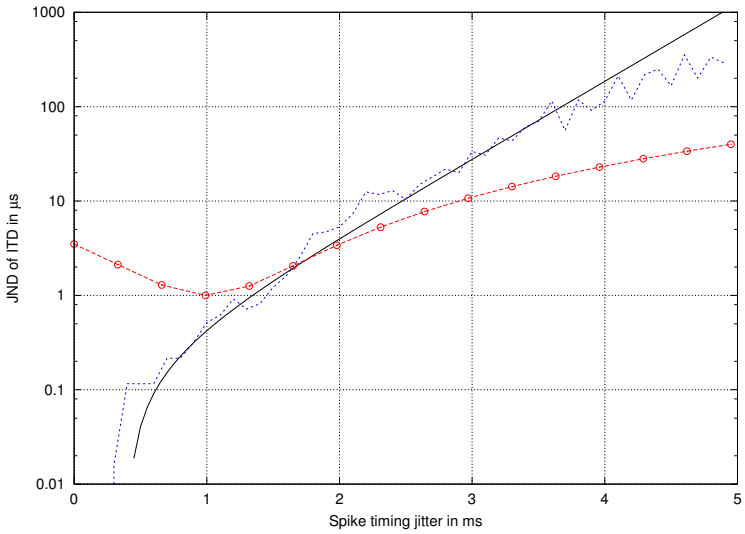

Figure 3: **The JND values in basic parameter set in dependence on the jitter magnitude.** This plot in semi-logarithmic y-scale shows just noticeable difference of interaural time difference depending on variation of the spike timing jitter. Jagged line: simulated data, solid line: an exponential fit to the simulations under the assumption of arbitrary time precision in the model circuit, line with circles: a quadratic function estimate of spike timing precision in a system with realistic noise.

Goldberg, J. M., Brown, P. B., 1969. Response of binaural neurons of dog superior olivary complex to dichotic tonal stimuli: Some physiological mechanisms of sound localization. J. Neurophysiol. 32 (4), 613–636.

Grothe, B., Pecka, M., McAlpine, D., 2010. Mechanisms of sound localization in mammals. Physiol. Rev. 90 (3), 983–1012.

Jeffress, L. A., 1948. A place theory of sound localization. J. Comp. Physiol. Psychol. 41 (1), 35–39.

Joris, P. X., Van de Sande, B., Louage, D. H., van der Heijden, M., 2006. Binaural and cochlear disparities. Proc. Natl. Acad. Sci. USA 103 (34), 12917–12922.

Joris, P. X., Yin, T. C., 1995. Envelope coding in the lateral superior olive. I.Sensitivity to interaural time differences. J. Neurophysiol. 73 (3), 1043–1062.

Joris, P. X., 1996. Envelope coding in the lateral superior olive. II.Characteristic delays and comparison with the responses in the medial superior olive. J. Neurophysiol. 76 (4), 2137–56.

Joris, P. X., Yin, T. C., 1998. Envelope coding in the lateral superior olive. III.Comparison with afferent pathways. J. Neurophysiol. 79 (1), 253–69.

Kopco, N., Huang, S., Belliveau, J. W., Raij, T., Tengshe, C., Ahveninen, J., 2012. Neuronal representations of distance in human auditory cortex. Proc. Natl. Acad. Sci. USA 109 (27), 11019–11024.

Kostal, L., Marsalek, P., 2010. Neuronal jitter: can we measure the spike timing dispersion differently? Chinese J Physiol 53 (6), 454–464.

Koutsou, A., Christodoulou, C., Bugmann, G., Kanev, J., 2012. Distinguishing the causes of firing with the membrane potential slope. Neural Comput. 24 (9), 2318–2345.

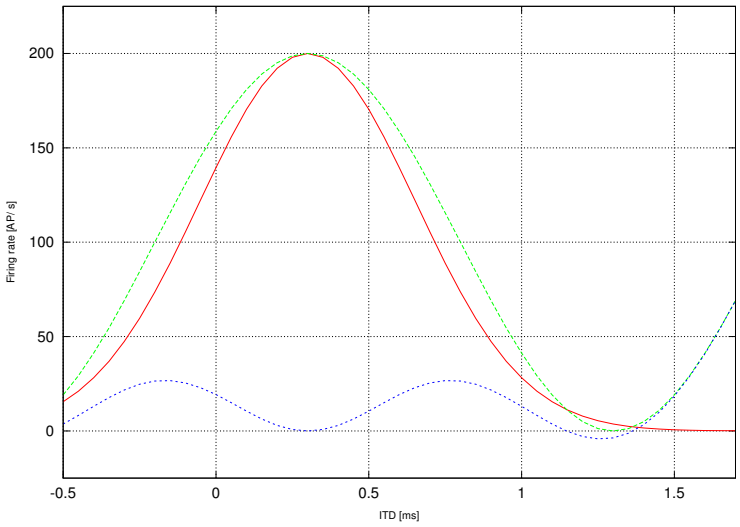

Figure 4: **Gaussian fit of the ITD to firing rate sloping calibration curve.** X-axis shows ITD in ms and y-axis shows corresponding firing rate in action potentials per second. Note that the curve peak is offset from the origin of coordinates at $t_{ITD} = 0$.

Krips, R., Furst, M., 2009. Stochastic properties of auditory brainstem coincidence detectors in binaural perception. J. Acoust. Soc. Am. 125 (3), 1567–1583.

Laback, B., Majdak, P., 2008. Binaural jitter improves interaural time-difference sensitivity of cochlear implantees at high pulse rates. Proc. Natl. Acad. Sci. USA 105 (2), 814–817.

Marsalek, P., 2000. Coincidence detection in the Hodgkin-Huxley equations. Biosystems 58 (1-3), 83–91.

Marsalek, P., 2001. Neural code for sound localization at low frequencies. Neurocomputing 38-40 (1-4), 1443–1452.

Marsalek, P., Kofranek, J., 2004. Sound localization at high frequencies and across the frequency range. Neurocomputing 58-60, 999–1006.

Marsalek, P., Kofranek, J., 2005. Spike encoding mechanisms in the sound localization pathway. Biosystems 79 (1-3), 191–8.

Marsalek, P., Lansky, P., 2005. Proposed mechanisms for coincidence detection in the auditory brainstem. Biol. Cybern. 92 (6), 445–451.

Mills, A. W., 1958. On the minimum audible angle. J. Acoust. Soc. Am. 30 (4), 237–246.

Mlynarski, W., Jost, J., 2014. Statistics of natural binaural sounds. PLoS One 9 (10), e108968, 1–15.

Reed, M. C., Blum, J. J., Mitchell, C. C., 2002. Precision of neural timing: Effects of convergence and time-windowing. J. Comput. Neurosci. 13 (1), 35–47.

Salinas, E., Sejnowski, T. J., 2000. Impact of correlated synaptic input on output firing rate and variability in simple neuronal models. J. Neurosci. 20 (16), 6193–6209.

Sanda, P., 2011. Jitter effect on the performance of the sound localization model of medial superior olive neural circuit. Eur. J. Biomed. Informatics 7 (1), 51–54.

Sanda, P., Marsalek, P., 2012. Stochastic interpolation model of the medial superior olive neural circuit. Brain Res. 1434, 257–265.

Simmons, J. A., 1989. A view of the world through the bat's ear: The formation of acoustic images in echolocation. Cognition, 155–199.

Smith, P. H., Joris, P. X., Yin, T. C. T., 1993. Projections of physiologically characterized spherical bushy cell axons from the cochlear nucleus of the cat: Evidence for delay lines to the medial superior olive. J. Comp. Neurol. 331 (2), 245–260.

Szalisznyo, K., Zalanyi, L., 2004. Role of hyperpolarization-activated conductances in the auditory brainstem. Neurocomputing 58, 401–407.

Tollin, D. J., 2003. The lateral superior olive: A functional role in sound source localization. Neuroscientist 9 (2), 127–143.

Toth, P. G., Marsalek, P., 2015. Analytical description of coincidence detection synaptic mechanisms in the auditory pathway. BioSystems 136, 90–98.

Toth, P. G., Marsalek, P., Pokora, O., 2017. Ergodicity and parameter estimates in auditory neural circuits. Submitted to Biol. Cybern.

Zwislocki, J., Feldman, R., 1956. Just noticeable differences in dichotic phase. J. Acoust. Soc. Am. 28 (5), 860–864.